

Published in final edited form as:

Nat Chem. 2021 November 01; 13(11): 1126–1132. doi:10.1038/s41557-021-00789-w.

Prebiotic photoredox synthesis from carbon dioxide and sulfite

Ziwei Liu¹, Long-Fei Wu¹, Corinna L. Kufner², Dimitar D. Sasselov², Woodward W. Fischer³, John D. Sutherland^{1,*}

¹MRC Laboratory of Molecular Biology, Francis Crick Avenue, Cambridge Biomedical Campus, Cambridge, CB2 0QH, UK

²Harvard-Smithsonian Center for Astrophysics, Cambridge, Massachusetts, MA 02138, USA

³Division of Geological and Planetary Sciences, California Institute of Technology, Pasadena, CA 91125, USA

Abstract

Carbon dioxide (CO₂) is the major carbonaceous component of many planetary atmospheres, including the Earth throughout its history. Carbon fixation chemistry— that reduces CO₂ to organics—utilizing hydrogen as stoichiometric reductant usually requires high pressures and temperatures, and yields of products of potential use to nascent biology are low. Here we demonstrate efficient ultraviolet photoredox chemistry between CO₂ and sulfite that generates organics and sulfate. The chemistry is initiated by electron photodetachment from sulfite giving sulfite radicals and hydrated electrons, which reduce CO₂ to its radical anion. A network of reactions—generating citrate, malate, succinate and tartrate by irradiation of glycolate in the presence of sulfite—was revealed. The simplicity of this carboxysulfitic chemistry and the widespread occurrence and abundance of its feedstocks suggest that it could have readily taken place on the surfaces of rocky planets. The availability of the carboxylate products on early Earth could have driven the development of central carbon metabolism before the advent of biological CO₂ fixation.

Many CO₂ reduction reactions have been discussed in the context of prebiotic chemistry, but all are problematic in that they require very special conditions and/or materials that are simply rare on planetary surfaces. For example, reduction by hydrogenation of bicarbonate (HCO₃⁻) over a Ni-Fe alloy under hydrothermal conditions¹ requires high temperatures and pressures, and predominantly generates the C₁ product methane, a poor feedstock for elaboration into (proto)biomolecules. By separating H₂ and CO₂ with a thin Fe(Ni)S precipitate barrier across which there is a large pH difference, milder conditions enable reduction, but the product formate (HCO₂⁻) is only produced in trace amounts². Reduction

Users may view, print, copy, and download text and data-mine the content in such documents, for the purposes of academic research, subject always to the full Conditions of use: <https://www.springernature.com/gp/open-research/policies/accepted-manuscript-terms>

*Correspondence to: johns@mrc-lmb.cam.ac.uk.

Author contributions Z.L. discovered this carboxysulfitic chemistry and explored its scope under the supervision of J.D.S. and with the assistance of L.-F.W., C.L.K. performed the pump-probe experiments under the supervision of D.D.S., W.W.F. evaluated the geochemical relevance of the chemistry. All authors co-wrote the manuscript.

Competing Interests The authors declare no competing interests.

of CO₂ using metallic Fe powder in water generates acetate, methanol, formate and pyruvate – the latter only transiently – but the widespread occurrence of Fe powder on rocky planets such as early Earth or Mars is unlikely³. Finally, UV photoreduction of CO₂ on colloidal ZnS semiconductor particles using hydrogen sulfide/hydrosulfide (H₂S/HS⁻) as a hole scavenger gives formate, acetate and propionate in low yield⁴, but these conditions are not likely to be common in a planetary context.

We previously demonstrated that hydrogen cyanide (HCN) can be reductively homologated using hydrated electrons (and/or hydrogen atoms derived therefrom by protonation) generated by UV irradiation of sulfidic anions in a process we termed cyanosulfidic chemistry^{5–6}. For this chemistry, we originally used H₂S/HS⁻ as stoichiometric reductant, but switched to using bisulfite⁷ (HSO₃⁻, pK_a ~7.2)/SO₃²⁻ because sulfur dioxide (SO₂) and H₂S are outgassed in a ~10:1 or greater ratio on Earth^{8–9}, and there is substantial evidence from the geological records of both Earth and Mars via the anomalous mass fractionation of sulfur isotopes that these sulfur species were important constituents of the early sulfur cycle^{10–11}. The Henry's law constant for SO₂ is greater than that of H₂S and the first pK_a of hydrated SO₂ (~1.9) is far lower than that of H₂S (~7.1)¹², so dissolution and hydration of SO₂ in surficial water followed by dissociation would therefore have been greater than dissolution and dissociation of H₂S on early Earth and Mars. Based on reports that hydrated electrons generated by UV illuminating diamond surfaces reduce CO₂ to carbon monoxide (CO) in acidic aqueous solution¹³, and the aforementioned semiconductor UV photoreduction of CO₂, we now wondered if HSO₃⁻/SO₃²⁻ could serve as the source of hydrated electrons for CO₂ reduction by UV photodetachment¹⁴ (Supplementary Table 1). Given that alkaline lakes can simultaneously absorb atmospheric CO₂ and SO₂ to give HCO₃⁻ and SO₃²⁻ and a growing body of evidence that suggests that such lakes could have concentrated other prebiotically important species on early Earth and maybe Mars^{15–16}, we started to explore reduction chemistry at mildly alkaline pH.

Results

Photoredox CO₂ fixation reaction

We subjected an aqueous solution of the sodium salts of HCO₃⁻ **1** (50 mM) and SO₃²⁻ (100 mM) at pH = 9 to UV irradiation from Hg-lamps with principal emission at 254 nm in a standard laboratory UV photoreactor and analyzed the resultant mixture by ¹H-NMR spectroscopy, integrating signals relative to those of a subsequently added standard to quantitate products. After 4 hours irradiation, formate **2** (18 mM), hydroxymethanesulfonate **3** (200 μM), methanol **4** (200 μM), glycolate **5** (200 μM), acetate **6** (50 μM), tartronate **7** (600 μM), and malonate **8** (300 μM) had been produced alongside both *rac*- and *meso*-tartrate **9a** (30 μM) and **9b** (30 μM) (structures of products shown in Fig. 1, Supplementary Fig. 1). Sulfate was detected as a photoredox co-product¹⁴ by precipitation of barium sulfate upon addition of barium chloride under conditions where barium sulfite is soluble¹⁷. The bicarbonate-sulfite irradiation experiment was repeated using ¹³C-labelled HCO₃⁻ **1** to confirm that all the products were generated from the photoreduction of CO₂, and all product assignments were confirmed by spiking with authentic standards (Supplementary Fig. 1 and 2). Surprisingly, we were able to detect elemental hydrogen (H₂) by ¹H-NMR

spectroscopy ($\delta = 4.5$ ppm) if it was generated *in situ* by performing the irradiation experiment in a quartz NMR tube. This peak decreased/disappeared simply by shaking the NMR tube presumably because this accelerated degassing. The signal assignment for H_2 was confirmed by running an NMR spectrum of the products of mixing zinc with hydrochloric acid solution in an NMR tube (Supplementary Fig. 3). Taken together, these results show that HCO_3^- **1** is reductively converted to C_2 , C_3 and (traces of) C_4 compounds as well as being reduced to other C_1 compounds in a process that also generates H_2 and SO_4^{2-} . If the initial concentration of HCO_3^- **1** was reduced to 5 mM and the concentration of SO_3^{2-} reduced to 10 mM, formate **2** (30 μM), glycolate **5** (20 μM), acetate **6** (10 μM), tartrate **7** (120 μM), and malonate **8** (30 μM) were observed by ^1H -NMR spectroscopy after 4 hours irradiation. The combined yield of organics in these experiments exceeded 10% demonstrating the remarkably high efficiency of this chemistry compared to other potentially prebiotic CO_2 fixation processes (Supplementary Fig. 4, Extended Data Fig. 1). The results were similar in experiments starting from carbon dioxide instead of sodium bicarbonate (Supplementary Fig. 5). In addition to the protiated products observed by ^1H -NMR spectroscopy, oxalate **10** was observed by ^{13}C -NMR spectroscopy in yields as high as 11% (Supplementary Fig. 6). At higher concentrations of reactants, the yield of C_1 products, especially formate **2**, went up relative to the yield of $\text{C}_{>1}$ products and after prolonged irradiation, a new C_3 product, β -hydroxypropionate **11** was identified (Supplementary Fig. 7).

Mechanistic study of the photoredox CO_2 fixation reaction network

We next investigated the photoreaction of the various products and some putative intermediates in the presence of SO_3^{2-} with a view to gaining information concerning the mechanism of the fixation chemistry. The results – summarized in Extended Data Fig. 2 (Supplementary Figs. 8 – 19) – can be rationalized by a reaction network based on photoredox radical chemistry (Fig. 1). Photodetachment of an electron from SO_3^{2-} gives a hydrated electron and a sulfite radical ($\cdot\text{SO}_3^-$)¹⁴. At pH 9, both loss of hydroxide from HCO_3^- **1** and loss of water from its conjugate acid, H_2CO_3 , furnish CO_2 . The latter process is efficiently catalyzed by nucleophiles^{18–20}, especially sulfite²¹, so it is unlikely that the otherwise slow kinetics of equilibration limit the photoredox chemistry. Although the equilibrium concentration of CO_2 is very low in a solution containing HCO_3^- **1** at pH = 9 relative to the concentration of **1** (Supplementary Fig. 20a)²², the rate constant for reaction of CO_2 with hydrated electrons to give the carboxyl radical **12** is extremely high²³ and the rate greatly exceeds the rate for protonation of hydrated electrons by **1** giving hydrogen atoms²⁴. The carboxyl radical **12** can either be reduced by hydrogen atom transfer (HAT) from HSO_3^- , which has a ~1% abundance relative to SO_3^{2-} at pH = 9, to give formate **2**, or undergo dimerization to give oxalate **10**, both directly and indirectly²⁵. Focussing on the chemistry of formate **2** first, one electron reduction, though relatively slow²⁶, gives the radical anion **13** and thence, through acid-base and hydration equilibria, the radicals **14** and **15** (although the latter is unfavoured relative to **13** and **14**). The radicals **13** and **14** have two main fates; reduction by HAT from HSO_3^- , or recombination with the carboxyl radical **12**. Coupled with acid-base and hydration equilibria, the first process (shown only for **13**), generates formaldehyde **16** and its hydrate **17** and the second (shown only for **14**) generates glyoxylate **18** via its hydrate **19**. Formaldehyde **16**, in equilibrium with the bisulfite adduct

3, can be reduced to the radical **20** which gives methanol **4** by HAT and glycolate **5** by recombination with the carboxyl radical **12**²⁷. Another major reaction of formate **2** is oxidation back to carboxyl radicals **12** by reaction with sulfite radicals. This is inferred from the observation that irradiation of formate **2** and SO_3^{2-} gives significant amounts of what appear to be products deriving from oxalate **10** in addition to C_1 products (Extended Data Fig. 2).

The other initial product of the carboxyl radical **12** – its dimer oxalate **10** – can be reduced by addition of a hydrated electron to give the radical anion **21**²⁸. This reduction is much faster than the corresponding reduction of formate **2** (Ultrafast pump-probe experiments and discussion are in Method). The radical anion **21** can undergo HAT leading to glyoxylate hydrate **19**, or recombination with another carboxyl radical **12** to give mesoxalate hydrate **22**, which equilibrates with mesoxalate **23**²⁹. Reduction of mesoxalate **23** by addition of a hydrated electron, or electron transfer from a carboxyl radical **12**, followed by HAT gives tartronate **7** and deoxygenation of the latter followed by HAT gives malonate **8**. In the same multistep way that formate **2** can be reduced to methanol **4**, reduction of one of the carboxylate groups of malonate **8** leads to β -hydroxypropionate **11**. Reduction of glyoxylate **18** (in equilibrium with the hydrate **19** and a bisulfite adduct)³⁰ and protonation of the initially formed radical anion³¹ leads to the key hydroxy-carboxymethyl radical **24** ($\text{pK}_a \sim 8.8$)³² which can recombine with the carboxyl radical **12** to give tartronate **7**, dimerize to give the tartrates **9**, or undergo HAT to give glycolate **5**. Deoxygenation of glycolate **5** gives the carboxymethyl radical **25**, which by recombination with the carboxyl radical **12** can give malonate **8**³³ and by HAT, acetate **6**.

Finally, we identified a number of photochemical steps other than the photodetachment of electrons from SO_3^{2-} , which initiates the reaction network. Norrish type I reactions of glyoxylate **18** and mesoxalate **23** generate radicals **12**, **15** and **26** (similar photocleavage of malonsemialdehyde **27**, en route to β -hydroxypropionate **11**, would generate radicals **15** and **25**) and photodetachment of an electron from oxalate **10**^{34–35} gives radical **28** which is thought to decarboxylate to the carboxyl radical **12**. These additional photochemical steps set up futile cycles in the network, but also forge links from the $\text{C}_{>1}$ parts of the network to the C_1 part (Supplementary Figs. 21 – 26).

Based on the foregoing analysis, we thought that it might be possible to increase the amount of the $\text{C}_{>1}$ products by adding sulfite portionwise – this would ensure that at any one time, the concentration of HSO_3^- would be low, so reaction flux through oxalate **10** would be favoured, but overall, there would be more reduction capacity. In accordance with expectation, at the end of this experiment, the combined yield of $\text{C}_{>1}$ products (>25%) greatly exceeded C_1 products (<1%) and the combined yield of malonate **8** (16.2%) and acetate **6** (1.0%) was greater than twice that of tartronate **7** (6.6%) and glycolate **5** (0.8%). Unexpectedly, a new product, sulfoacetate **29** (0.8%) was formed in low yield, presumably through recombination of carboxymethyl radicals **25** with sulfite radicals. (Supplementary Fig. 27, Extended Data Fig. 1, Entry 6). The general features of the time course of the CO_2 reduction network were also revealed by this experiment. After 1 hour, formate **2** was the major product accompanied by traces of glycolate **5** and tartronate **7**. After 2 hours, the

amount of formate **2** had decreased and glycolate **5** and tartronate **7** were now the major products along with smaller amounts of acetate **6** and malonate **8**. After further irradiation, the levels of formate **2**, glycolate **5** and tartronate **7** stayed at about the same level and malonate **8** became the major product with minor amounts of acetate **6** and methanol **4**. This time course behaviour can be understood from the reaction network (Fig. 1). At the outset of the experiment, the only carbonaceous species for the hydrated electrons to reduce is CO₂. Carboxyl radicals **12** thereby produced apparently undergo HAT from HSO₃⁻ faster than they dimerise, and so formate **2** increases. However, the conversion of carboxyl radicals **12** to **2** is reversible, and so after some time a sufficient amount of oxalate **10** is produced for it to be reduced by the hydrated electrons as well. The reduction of oxalate **10** is much faster than the reduction of formate **2** (investigated by ultrafast pump-probe spectroscopy and further discussed in Methods), so **2** is consumed at the expense of making reduction products of **10**. The appearance of the radical anion **21** opens up a new path for consumption of carboxyl radicals **12**, including recombination to give mesoxalate hydrate **22** that is rapidly converted to tartronate **7** and a new path for the consumption of HSO₃⁻, namely HAT to **21** giving glyoxylate **18** and thence, through rapid further reduction, glycolate **5**. The opening of these new reaction paths reduces the level of formate **2** to a steady state where its consumption is balanced by continuous production from CO₂ via carboxyl radicals **12**. Eventually, the deoxygenation of tartronate **7** coupled to the slow reduction of malonate **8** means that the latter becomes the predominant product. At higher initial concentrations of sulfite, the early formate **2** pulse lasts longer and produces higher early amounts of **2**, but eventually the paths to C_{>1} products start to operate and levels of formate **2** drop. Even if formate **2** is reduced, the reversibility of the downstream steps to C₁ products and other paths from the C₁ part of the network to the C_{>1} part means that products more complex than **2** eventually accumulate.

It has been reported that CO₂ can be reduced to CO with hydrated electrons produced by UV irradiation of diamond in the presence of bisulfite as hole scavenger at pH = 3.2¹³. The carboxyl radical **12** is formed as in our chemistry, but absent the chromophoric sulfite acting to absorb UV, it is photolyzed³⁶ to CO and O⁻, the conjugate base of the hydroxyl radical, which is then reduced by bisulfite. Hydrogen was not observed as a product because the reaction was carried out under a sufficiently high concentration of CO₂ to out-compete H⁺ in reaction with electrons.

Glycolate photoredox reaction

As we investigated the photoreactions of the products and putative intermediates of the CO₂ reduction network with SO₃²⁻, the photoredox chemistry of one product – glycolate **5** – stood out. Acetate **6** (16.2 mM), malonate **8** (0.1 mM), sulfoacetate **29** (7.8 mM), citrate **30** (0.2 mM), *rac*-tartrate **9a** (1.5 mM), *meso*-tartrate **9b** (1.0 mM), malate **31** (2.9 mM), succinate **32** (1.1 mM) and hydroxycitrate **33** (0.19 mM) along with C₁ products were detected by ¹H-NMR spectroscopy after 6 hours irradiation of glycolate **5** (50 mM) and SO₃²⁻ (100 mM) (Supplementary Fig. 12, Extended Data Fig. 2, Entry 4). Particularly noteworthy is the fact that citrate **30**, malate **31** and succinate **32** are key constituents of the Krebs cycle – a major cycle of central carbon metabolism, the consequences of which are discussed below. Remarkably, when the concentration of glycolate **5** was reduced to

5 mM and the concentration of SO_3^{2-} reduced to 10 mM, after 2 hours irradiation, C_1 products were no longer detected but the higher products were still formed in a comparable overall yield albeit with a different relative abundance distribution (Supplementary Fig. 13, Extended Data Fig. 2, Entry 5). The chemistry that generates acetate **6**, malonate **8** and the tartrates **9** is the same as some of that of the CO_2 fixation reaction network, but additional reactions now contribute to the detectable products (Fig. 2). Abstraction of a hydrogen atom from glycolate **5** by a sulfite radical generates the hydroxy-carboxymethyl radical **24** whilst redox compensatory reduction of **5** generates the carboxymethyl radical **25**. Dimerization of **24** produces the tartrates **9** whereas dimerization of **25** produces succinate **32** as well as acetate **6** and glycolate **5**³⁷. Recombination of radicals **24** and **25** provides one route to malate **31**, a second would be from reduction of **9**. Similar reduction of malate **31** would give a second path to succinate **32**. Oxidation of the tartrates **9** and malate **31** to the corresponding hydroxyalkyl radicals **34** and **35** followed by recombination of these radicals with radicals **24** or **25** would give dihydroxycitrate **36**, hydroxycitrate **33** and citrate **30**. Reduction of **36** would constitute another reaction channel to hydroxycitrate **33** and further reduction of **33**, another channel to citrate **30**. In contrast to the reaction network starting from CO_2 where all products are reduced relative to the starting material, the network starting from glycolate **5** is more subtle and contains both carbon oxidations and reductions. Thus malate **31** and citrate **30** are at the same oxidation level as glycolate **5**, succinate **32** and acetate **6** are more reduced and the tartrates **9** and hydroxycitrate **33** are, on average, more oxidized.

Photoredox reactions under lower photon flux

We also evaluated the bicarbonate reduction chemistry using a less intense broadband UV source, StarLab³⁸ - an in-house constructed photoreactor designed to deliver UV radiation with a wavelength distribution representative of that from the Sun incident on the surface of early Earth, at a ~100 fold higher intensity than the Sun in a quiescent state and ~10 fold lower intensity than that during maximum flaring. After irradiation for 7 days in this apparatus, an aqueous solution of the sodium salts of HCO_3^- **1** (5 mM) and SO_3^{2-} (50 mM) at pH = 9 gave a mixture of protiated products similar to that obtained upon higher intensity irradiation in the standard laboratory photoreactor (at 254 nm for shorter time intervals) plus ethanol **37**, confirming the utility of using 254 nm UV light to study this chemistry (Supplementary Fig. 28, Extended Data Fig. 1, Entry 7). Oxalate **10** was also detected in a similar experiment using ^{13}C -labelled bicarbonate (Supplementary Fig. 29). Ethanol **37** could plausibly be obtained via dimerization of the hydroxymethyl radical **20** giving ethylene glycol **38**, dehydration of **38** through radical **39** and the enolxy radical **40**³⁹ to acetaldehyde **41** and reduction (Fig. 1). Alternatively, acetate **6** could be reduced to acetaldehyde **41** and thence ethanol **37**.

We then investigated the carboxysulfite photoredox chemistry of glycolate **5** in the StarLab photoreactor. After 8 hours irradiation of glycolate **5** (50 mM) and SO_3^{2-} (100 mM) with this less intense light source, acetate **6** (1.7 mM), sulfoacetate **29** (0.2 mM), *rac*-tartrate **9a** (0.4 mM), *meso*-tartrate **9b** (0.4 mM), malate **31** (0.2 mM), and succinate **32** (trace) along with C_1 products were detected by ^1H -NMR spectroscopy (Supplementary Fig. 14, Extended Data Fig. 2, Entry 6). Longer irradiation of more dilute samples of glycolate **5** (5

mM) and SO_3^{2-} (50 mM) in the StarLab photoreactor resulted in higher yields of the same species and additionally produced malonate **8** and hydroxypropionate **11** (Supplementary Fig. 30, Extended Data Fig. 2, Entry 7).

Discussion

Planetary relevance

An important aspect of this chemistry is that the conditions and materials necessary to foster carboxysulfidic carbon fixation (short wave UV light, CO_2 and SO_2 derived from volcanism, and bodies of standing and flowing water on the crust) are mild, widespread, and expected to be common on rocky planets. Notably, there is geological evidence from the rock records of Earth and Mars that these conditions were met early in their history. Oxygen isotope ratios from Hadean zircons^{40–41} and sedimentological observations from the earliest sedimentary record⁴² indicate abundant surface liquid water. Silicate weathering reactions occurred that sourced the alkalinity necessary to enable the dissociated hydrates, bicarbonate and sulfite, to partition from the atmosphere and accumulate in bodies of water in contact with the atmosphere⁴³. Moreover, the anomalous fractionation of multiple sulfur isotopes in the early geological record¹⁰ provides a direct measure of SO_2 photochemistry that establishes a valuable atmospheric correlate of the aqueous carbon fixation processes described herein. Finally, each of these observations for the early Earth that illustrates the plausibility of this chemistry occurring now has its complement in the Mars geological record^{11, 44–47}. Thus, the ingredients and basic conditions for carboxysulfidic chemistry to take place would have been present on both Earth and Mars. Depending on conditions, carboxylates such as formate **2**, oxalate **10** or acetate **6** and malonate **8** are likely to have been the major initial products. Decarboxylation of malonate **8** to acetate **6** occurs on a short geological timescale in solution (~10 years at neutral pH and at 25°C)⁴⁸ whereas oxalate **10** (in the absence of ferric ions and light)⁴⁹, like acetate **6** is long-term stable and so it seems likely that these latter two products would have become the most abundant $\text{C}_{>1}$ organics on early Earth had life not emerged – they might still be the most abundant organics on Mars if life did not emerge there.

The linkage between carboxysulfidic chemistry and cyanosulfidic chemistry

The case for conditions conducive to cyanosulfidic chemistry being present on both young planets has also been made⁵⁰. We note that for the full range of cyanosulfidic chemistry products to result, a scenario involving the mixing of bodies of water or flows (e.g. stream water) having subtly different reaction histories would probably be necessary. In locations where the basic conditions for cyanosulfidic chemistry were met, but the mixing of streams was absent or different, a limited set of products would have been generated and the first product of the restricted reaction network, glycolonitrile **42**, would probably have been the most widespread. In addition, glycolonitrile **42** could have resulted from reaction of HCN with formaldehyde **16** rained in after production in the upper atmosphere by photoreduction of CO_2 ⁵¹. Hydrolysis of the nitrile group of glycolonitrile **42**, however produced, generates glycolate **5**, which could be converted by subsequent carboxysulfidic chemistry to the range of carboxylate products previously described. (Fig. 3) As the hydrolysis of glycolonitrile **42** generates ammonia in addition to glycolate **5**, we also carried out the irradiation of **5** and

sulfite in the presence of ammonia. Ammonia did not affect the outcome of the photoredox chemistry – the same set of products was formed with or without ammonia (Supplementary Fig. 31).

Biochemical relevance

Use of the products of cyanosulfidic chemistry as building blocks by nascent biology would eventually lead to their environmental depletion and biology would then be under evolutionary pressure to synthesize these building blocks from anything else that happened to be available and usable. Biology could either spread to encounter these materials in their place of synthesis, or fluvial advection could move them to the location of biology. It is fascinating that the majority of the carboxylate products deriving from the carboxysulfitic chemistry of glycolate **5** are key nodes of central carbon metabolism in extant biology and it seems likely that their synthesis by carboxysulfitic chemistry set the stage for the development of this metabolic network. At first glance, tartrate **9** seems to be somewhat an outlier, but its dehydration would lead through an enol to oxaloacetate⁵³ and its oxidation, to dihydroxyfumarate which spontaneously decarboxylates to give glycolaldehyde⁵⁴, a precursor of higher sugars.

With time, supply of most of the products of the carboxysulfitic chemistry of glycolate **5** would also dwindle and biology would have to evolve to make do with simpler, more abundant carbonaceous materials in the environment. The major long term stable products of the carboxysulfitic chemistry of CO₂ – formate **2**, acetate **6** and oxalate **10** – could then provision central carbon metabolism through development of a pyruvate-formate lyase activity and the glyoxylate shunt of the Krebs cycle via reduction of oxalate **10** to glyoxylate **18**. Finally, even oxalate **10** and acetate **6** would become depleted and biology would be under evolutionary pressure to use the only remaining abundant carbon source, namely CO₂.

Methods

General Methods

All reagents and deuterated solvents used for reactions and spiking experiments were purchased from Sigma-Aldrich and were used without further purification. All photochemical reactions were carried out in *Norell* Suprasil quartz NMR tubes purchased from Sigma-Aldrich using Hg lamps with principal emission at 254 nm in a *Rayonet* photochemical chamber reactor RPR-200, acquired from The Southern New England Ultraviolet Company. StarLab is an in-house constructed photoreactor that delivers broadband UV-Vis (from 220 nm to ~750 nm by using water as an optical filter) irradiation to a sample from a 75W xenon lamp manufactured by Horiba³⁸. A *Mettler Toledo* SevenEasy pH Meter S20 was used to monitor the pH, and degassed H₂O or D₂O was achieved by four rounds of freeze-pump-thaw cycling. ¹H-, and ¹³C-nuclear magnetic resonance (NMR) spectra were acquired using a *Bruker* Ultrashield 400 Plus or *Bruker* Ascend 400 operating at 400.1, and 100.6 MHz, respectively. Samples consisting of H₂O/D₂O mixtures were analyzed using HOD suppression to collect ¹H-NMR data. Chemical shifts (δ) are shown in ppm. Coupling constants (J) are given in Hertz and the notations s, d, t represent the multiplicities singlet, doublet, and triplet. The conversion

yields were determined by relative integrations of the signals using a known amount of acetamide as internal reference in the ^1H -NMR spectrum.

General method of photoreaction of carboxylates with sulfite

Carboxylates and sodium sulfite (final concentrations were mentioned in Extended Data Fig. 1 and Extended Data Fig. 2) were dissolved in degassed $\text{H}_2\text{O}/\text{D}_2\text{O}$ (9:1, 0.5 mL). After the pH was adjusted to the reported value with NaOH/HCl, the mixture was transferred to a quartz NMR tube which was sealed and irradiated for the reported time (Extended Data Fig. 1 and Extended Data Fig. 2). The resultant solution was analysed by ^1H - and/or ^{13}C -NMR spectroscopy. The yield was calculated by spiking with 4,5-dicyanoimidazole (final concentration of 0.5 mM, 1 mM or 5 mM) and relative integration.

Preparing hydrogen gas in an NMR tube

Metallic zinc (~6 mg) was added to 0.5 mL HCl (0.1 M) aqueous solution. This solution was transferred to an NMR tube after being vortexed for 5 seconds, and was then analysed by ^1H -NMR spectroscopy.

Sulfate identification¹⁷

Sodium bicarbonate (21 mg, 0.25 mmol) and sodium sulfite (63 mg, 0.5 mmol) were dissolved in degassed water (10 mL) and the pH of the resultant solution was adjusted to 9 by adding NaOH/HCl solution. The mixture was then sealed in a quartz tube and irradiated with 254 nm light in the Rayonet photoreactor for 4 hours. 3 mL of the resulting solution was diluted to 20 mL with water and acidified to pH = 1 by the addition of concentrated HCl. The acidified solution was heated to nearly boiling for at least 30 min to remove all carbon dioxide and sulfur dioxide. Barium chloride solution was then added to the solution to give a precipitate which persisted upon boiling for another 30 min. The precipitate did not dissolve in dilute HCl solution.

Ultrafast pump-probe experiments

The general principles of pump-probe spectroscopy are described in the following references^{55–57}. The fundamental of the excitation pulses (800 nm) was generated by a Ti:Sa based laser-amplifier system (Solstice Ace by Spectra-Physics, Newport Co.) with a repetition rate of 1 kHz and a pulse duration of ~90 fs. The excitation pulses (251 nm) were generated in a nonlinear amplifier system (Topas Prime + NIRUVis, Light Conversion, Ltd.) and stretched by a 25 cm fused silica block (Corning) to ~1.7 ps to suppress two-photon ionization of the solvent. The excitation energy at the sample position was ~1 μJ and the spot diameter of ~250 μm (fwhm). For our *microsecond* ultrafast pump-probe spectroscopy (Supplementary Table 2) the broadband probe light (unpolarized) was generated, delayed, and detected in an EOS Fire system (Ultrafast Systems, LLC), with a nominal spectral range of 350 – 950 nm. For our *picosecond* ultrafast pump-probe spectroscopy (Supplementary Fig. 32) the broadband probe light was generated, delayed, and detected in a HELIOS Fire system (Ultrafast Systems, LLC), with a nominal spectral range of 400 – 750 nm. These spectral ranges are ideal for monitoring the broad absorption feature of the hydrated

electron, which is centered near 700 nm. The experiments were carried out at a temperature of 23°C.

The transient pump-probe data were cropped to the spectral range 450 nm – 913 nm and 20 adjacent channels were averaged (Surface Explorer, Ultrafast Systems, LLC). A global fitting analysis to determine transient lifetimes was performed^{58–60}.

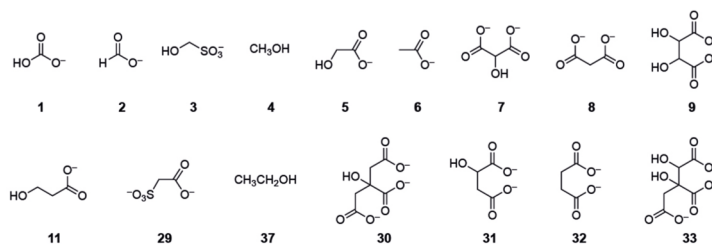
Ultrafast pump-probe spectroscopic investigation of reduction chemistry

The rate constant reported in the literature for reaction of hydrated electrons with formate **2** ($k = 2.4 \times 10^4 \text{ M}^{-1}\text{s}^{-1}$)²⁶ is considerably lower than that for reduction of oxalate (average of three values given in reference⁶¹ is $3.1 \times 10^7 \text{ M}^{-1}\text{s}^{-1}$). However, in our experiments, oxalate **10** is also prone to photoionization^{34–35} and so it was not clear if reaction of hydrated electrons with oxalate in our experiments is, or is not, faster than reaction of hydrated electrons with formate **2**. The rate constant for reaction of hydrated electrons with glycolate **5** ($k = 8.2 \times 10^6 \text{ M}^{-1}\text{s}^{-1}$)³² is high, although the authors of this paper caution that this “unexpectedly high value may be due to trace impurity in the sample”. Furthermore, although the rate constant for reaction of solvated electrons with CO_2 is known²³, we do not know the concentration of CO_2 in our experiments, or whether the catalysis of its interconversion with carbonic acid and bicarbonate by sulfite affects this rate. Accordingly, we used ultrafast pump-probe spectroscopy both to confirm the photoionization of oxalate **10** and compare it to that of sulfite (Supplementary Fig. 32A), and to measure hydrated electron decay kinetics in mixtures representative of the mixtures used in our continuous irradiation experiments (Supplementary Table 3). These pump-probe experiments confirmed the photoionization of oxalate **10** and further revealed that bicarbonate, formate **2** and glycolate **5** react at similar rates with hydrated electrons in our experiments, and that oxalate **10** reacts considerably faster (Supplementary Fig. 32 and Supplementary Tables 2 and 3).

Extended Data

Entry	[NaHCO ₃] /mM	[Na ₂ SO ₃] /mM	Products													Time
			2 ^a	3	4	5	6	7	8	9a	9b	11	29	37		
1	5	10	0.03 0.6 %			20 0.8 %	10 0.4 %	120 7.2 %	30 1.8 %							4 h
2	20	40	3.7 19 %		40 0.2 %	100 1.0 %	20 0.2 %	600 9.0 %	200 3.0 %							4 h
3	50	100	18.0 36 %	200 0.4 %	200 0.4 %	200 0.8 %	50 0.2 %	600 3.6 %	300 1.8 %	30 0.24 %	30 0.24 %					4 h
4	100	200	27.6 28 %	500 0.5 %	120 0.1 %	20 0.04 %	20 0.04 %	150 0.5 %	40 0.12 %							4 h
5 ^b	100	200	52.7 53 %	200 0.2 %	4600 4.6 %	300 0.6 %	300 0.6 %	500 1.5 %	900 2.7 %	30 0.12 %	20 0.08 %	100 0.3 %				24 h
6 ^c	5	4 × 10	0.03 0.6 %			20 0.8 %	27 1.0 %	110 6.6 %	270 16.2 %						20 0.8 %	4 × 1 h
7 ^d	5	50	1.6 32 %	15 0.3 %	143 2.9 %	12 0.5 %	8 0.3 %	59 3.5 %	102 6.1 %					8 0.3 %	45 1.8 %	168 h

Extended Data Fig. 1. Product concentrations and percentage yields after UV irradiation of solutions of NaHCO₃ and Na₂SO₃.



Entry	Reactant	Products														Time		
		2 ^a	3	4	5	6	7	8	9a	9b	11	29	30	31	32		33	37
1	2	32.1 ^b 64 %	1900 3.8 %	3300 6.6 %	300 1.2 %	240 1.0 %	340 2.0 %	550 3.3 %				70 0.28 %						
2	3	6.9 14 %	38000 ^b 76 %	4200 8.0 %		200 0.8 %												
3	4	1.4 2.8 %	2300 4.6 %	40000 ^b 80 %		273 1.09 %												1580 6.32 %
4	5	0.6 0.6 %	700 0.7 %	150 0.15 %	3500 ^b 7 %	16200 32 %		100 0.3 %	1500 ^d 6 %	1000 4 %		8000 16 %	200 1.2 %	3000 12 %	1070 4.4 %	190 1.1 %		
5	5 ^c			10 0.1 %	940 ^b 18 %	1000 20 %		40 1.2 %	380 ^d 15 %	190 7.6 %		810 16 %	15 0.9 %	390 15.6 %	70 2.8 %			
6	5 ^e	0.7 0.7 %	400 0.4 %	20 0.02 %	42500 ^b 85 %	1700 3.4 %			400 ^d 1.6 %	400 1.6 %		200 0.4 %		200 0.8 %				
7	5 ^{e,f}	0.89 8.9 %	35 0.35 %	40 0.4 %	945 ^b 19 %	356 7.12 %		15 0.45 %	210 ^d 8.4 %	105 4.2 %	50 1.5 %	130 2.6 %		50 2.0 %	5 0.2 %			
8	6			40 0.04 %	100 0.2 %	37000 ^b 74 %		30 0.09 %				1600 3.2 %			90 0.36 %			480 0.96 %
9	7	2.4 1.6 %					11200 ^b 22.4 %	24300 48.6 %	N.d. ^g	120 0.3 %	800 1.6 %	400 0.5 %						
10	8	0.4 0.3 %				200 0.3 %		46000 ^b 92 %				2000 4.0 %						
11	10	9.2 9.2 %		40 0.04 %	3700 7.4 %	100 0.2 %	200 6.0 %	50 0.15 %	1100 4.4 %	1100 4.4 %					300 1.2 %			

Extended Data Fig. 2. Product concentrations and percentage yields after irradiation of individual bicarbonate reduction products (50 mM) and Na₂SO₃ (100 mM).

Supplementary Material

Refer to Web version on PubMed Central for supplementary material.

Acknowledgements

The authors thank J.D.S., D.D.S. and W.W.F. group members for helpful discussions. This research was supported by the Medical Research Council (MC_UP_A024_1009 to J.D.S.), the Simons Foundation (290362 to J.D.S., 290360 to D.D.S. and 554187 to W.W.F.). C.L.K. and D.D.S. thank Wolfgang Zinth, Pablo Dominguez, Daniel Yahalomi, Gabriella Lozano for helpful discussions and experimental assistance, and acknowledge the Harvard Origins of Life Initiative.

Data availability

All data generated or analysed during this study are included in the manuscript and the Supplementary Information.

References

- Horita J, Berndt ME. Abiogenic methane formation and isotopic fractionation under hydrothermal conditions. *Science*. 1999; 285 :1055–1057. [PubMed: 10446049]
- Hudson R, et al. CO₂ reduction driven by a pH gradient. *Proc Natl Acad Sci USA*. 2020; 117 :22873–22879. [PubMed: 32900930]

3. Varma SJ, Muchowska KB, Chatelain P, Moran J. Native iron reduces CO₂ to intermediates and end-products of the acetyl-CoA pathway. *Nature Ecol Evol.* 2018; 2 :1019–1024. [PubMed: 29686234]
4. Zhang XV, et al. Photodriven reduction and oxidation reactions on colloidal semiconductor particles: Implications for prebiotic synthesis. *J Photochem Photobiol Chem.* 2007; 185 :301–311.
5. Patel BH, Percivalle C, Ritson DJ, Duffy CD, Sutherland JD. Common origins of RNA, protein and lipid precursors in a cyanosulfidic protometabolism. *Nat Chem.* 2015; 7 :301–307. [PubMed: 25803468]
6. Green NJ, Xu J, Sutherland JD. Illuminating life's origins: UV photochemistry in abiotic synthesis of biomolecules. *J Am Chem Soc.* 2021; 143 7219 [PubMed: 33880920]
7. Xu J, et al. Photochemical reductive homologation of hydrogen cyanide using sulfite and ferrocyanide. *Chem Commun.* 2018; 54 :5566–5569.
8. Zahnle K, Claire M, Catling D. The loss of mass-independent fractionation in sulfur due to a Palaeo-proterozoic collapse of atmospheric methane. *Geobiology.* 2006; 4 :271–283.
9. Gerlach TM. Evaluation and restoration of the 1970 volcanic gas analyses from Mount Etna, Sicily. *J Volcanol. Geotherm Res.* 1979; 6 :165–178.
10. Farquhar J, Bao H, Thiemens M. Atmospheric influence of Earth's earliest sulfur cycle. *Science.* 2000; 289 :756–758. [PubMed: 10926533]
11. Farquhar J, Savarino J, Jackson T, Thiemens MH. Evidence of atmospheric sulphur in the martian regolith from sulphur isotopes in meteorites. *Nature.* 2000; 404 :50–52. [PubMed: 10716436]
12. Ranjan S, Todd ZR, Sutherland JD, Sasselov DD. Sulfidic anion concentrations on early earth for surficial origins-of-life chemistry. *Astrobiology.* 2018; 18 :1023–1040. [PubMed: 29627997]
13. Zhang L, Zhu D, Nathanson GM, Hamers RJ. Selective photoelectrochemical reduction of aqueous CO₂ to CO by solvated electrons. *Angew Chem Int Ed.* 2014; 126 :9904–9908.
14. Fischer M, Warneck P. Photodecomposition and photooxidation of hydrogen sulfite in aqueous solution. *J Phys Chem.* 1996; 100 :15111–15117.
15. Toner JD, Catling DC. A carbonate-rich lake solution to the phosphate problem of the origin of life. *Proc Natl Acad Sci USA.* 2020; 117 :883–888. [PubMed: 31888981]
16. Toner JD, Catling DC. Alkaline lake settings for concentrated prebiotic cyanide and the origin of life. *Geochim Cosmochim Acta.* 2019; 260 :124–132.
17. Malati, MA. Experimental inorganic/physical chemistry: an investigative, integrated approach to practical project work. Woodhead Publishing Limited; 1999.
18. Murphy LJ, et al. A simple complex on the verge of breakdown: isolation of the elusive cyanofornate ion. *Science.* 2014; 344 (6179) :75–78. [PubMed: 24700853]
19. Hering C, von Langermann J, Schulz A. The elusive cyanofornate: an unusual cyanide shuttle. *Angew Chem Int Ed.* 2014; 53 :8282–8284.
20. Juhl M, Petersen AR, Lee J-W. CO₂-enabled cyanohydrin synthesis and facile iterative homologation reactions. *Chem Eur J.* 2021; 27 :228–232. [PubMed: 32812672]
21. Roughton FJW, Booth VH. The catalytic effect of buffers on the reaction CO₂ + H₂O = H₂CO₃. *Biochem J.* 1938; 32 :2049–2069. [PubMed: 16746846]
22. Zeebe, RE, Wolf-Gladrow, D. CO₂ in seawater: equilibrium, kinetics, isotopes. Vol. 65. Gulf Professional Publishing; 2001.
23. Gordon S, Hart EJ, Matheson MS, Rabani J, Thomas JK. Reactions of the hydrated electron. *Discussions Faraday Soc.* 1963; 36 :193–205.
24. Hentz RR, Farhataziz, Milner DJ, Burton M. γ -Radiolysis of liquids at high pressures. III. Aqueous solutions of sodium bicarbonate. *J Chem Phys.* 1967; 47 :374–377.
25. Flyunt R, Schuchmann MN, von Sonntag C. A common carbanion intermediate in the recombination and proton-catalysed disproportionation of the carboxyl radical anion CO₂⁻ in aqueous solution. *Chem Eur J.* 2001; 7 :796–799. [PubMed: 11288870]
26. Swallow AJ. Recent results from pulse radiolysis. *Photochem Photobiol.* 1968; 7 :683–694.
27. Getoff N, Gütlbauer F, Schenck GO. Strahlenchemische carboxylierung von ameisenäure und methanol in wässriger lösung. *Int J Appl Radiat Isot.* 1966; 17 :341–349. [PubMed: 5962663]
28. Getoff N, Schwörer F, Markovic VM, Sehested K, Nielsen SO. Pulse radiolysis of oxalic acid and oxalates. *J Phys Chem.* 1971; 75 :749–755.

29. Doussin J-F, Monod A. Structure-activity relationship for the estimation of OH-oxidation rate constants of carbonyl compounds in the aqueous phase. *Atmos Chem Phys*. 2013; 13 :11625–11641.
30. Olson TM, Hoffmann MR. Formation kinetics, mechanism and thermodynamics of glyoxylic acid-S(IV) adducts. *J Phys Chem*. 1988; 92 :4246–4253.
31. Laroff GP, Fessenden RW. ¹³C Hyperfine interactions in radicals from some carboxylic acids. *J Chem Phys*. 1971; 55 :5000–5008.
32. Bell JA, Grunwald E, Hayon E. Kinetics of deprotonation of organic free radicals in water Reaction of HOC·HCO₂⁻, HOC·HCONH₂ and HOC·CH₃CONH₂ with various bases. *J Am Chem Soc*. 1975; 97 :2995–3000.
33. Getoff N. CO₂ and CO utilization: radiation-induced carboxylation of aqueous chloroacetic acid to malonic acid. *Radiat Phys Chem*. 2003; 67 :617–621.
34. Arvis M, Lustig H, Hickel B. Étude par photolyse éclair de la photoionisation des anions formiate, acetate et oxalate dans l'eau. *J Photochem*. 1980; 13 :223–232.
35. Huie RE, Clifton CL. Kinetics of the reaction of the sulfate radical with the oxalate anion. *Int J Chem Kinetics*. 1996; 28 :195–199.
36. Habteyes T, Velarde L, Sanov A. Photodissociation of CO₂⁻ in water clusters via Renner-Teller and conical interactions. *J Chem Phys*. 2007; 126 154301 [PubMed: 17461620]
37. Wang W-F, Schuchmann MN, Schuchmann H-P, von Sonntag C. The importance of mesomerism in the termination of α-carboxymethyl radicals from aqueous malonic and acetic acids. *Chem Eur J*. 2001; 7 :791–795. [PubMed: 11288869]
38. Rimmer P, et al. Timescales for prebiotic photochemistry under realistic surface UV conditions. *Astrobiology* Accepted.
39. Gilbert BC, Larkin JP, Norman ROC. Electron spin resonance studies Part XXXIII Evidence for heterolytic and homolytic transformations of radicals from 1,2-diols and related compounds. *J Chem Soc, Perkin Trans*. 1972; 2 :794–802.
40. Wilde S, Valley J, Peck W, Graham CM. Evidence from detrital zircons for the existence of continental crust and oceans on the Earth 4.4 Gyr ago. *Nature*. 2001; 409 :175–178. [PubMed: 11196637]
41. Valley JW, et al. 4.4 billion years of crustal maturation: oxygen isotope ratios of magmatic zircon. *Contrib Mineral Petrol*. 2005; 150 :561–580.
42. Rosing MT. ¹³C-Depleted carbon microparticles in >3700-Ma sea-floor sedimentary rocks from west Greenland. *Science*. 1999; 283 :674–676. [PubMed: 9924024]
43. Kasting JF. The Goldilocks planet? How silicate weathering maintains Earth “just right”. *Elements: An International Magazine of Mineralogy, Geochemistry, and Petrology*. 2019; 15 :235–240.
44. Grotzinger JP, et al. Deposition, exhumation, and paleoclimate of an ancient lake deposit, Gale crater, Mars. *Science*. 2015; 350 doi: 10.1126/science.aac7575
45. DiBiase RA, Limaye AB, Scheingross JS, Fischer WW, Lamb MP. Deltaic deposits at Aeolis Dorsa: sedimentary evidence for a standing body of water on the northern plains of Mars. *J Geophys Res Planets*. 2013; 118 :1285–1302.
46. Hurowitz JA, et al. Redox stratification of an ancient lake in Gale Crater, Mars. *Science*. 2017; 356 doi: 10.1126/science.aah6849
47. Milliken RE, Fischer WW, Hurowitz JA. Missing salts on early Mars. *Geophys Res Letts*. 2009; 36 doi: 10.1029/2009GL038558
48. Wolfenden R, Lewis CA Jr, Yuan Y. Kinetic challenges facing oxalate, malonate, acetoacetate and oxaloacetate decarboxylases. *J Am Chem Soc*. 2011; 133 :5683–5685. [PubMed: 21434608]
49. Goldstein S, Rabani J. The ferrioxalate and iodide-iodate actinometers in the UV region. *J Photochem Photobiol A*. 2008; 193 :50–55.
50. Sasselov DD, Grotzinger JP, Sutherland JD. The origin of life as a planetary phenomenon. *Sci Adv*. 2020; 6 doi: 10.1126/sciadv.aax3419
51. Cleaves HJ II. The prebiotic geochemistry of formaldehyde. *Precambrian Res*. 2008; 164 :111–118.

52. Liu Z, Wu LF, Xu J, Bonfio C, Russell DA, Sutherland JD. Harnessing chemical energy for the activation and joining of prebiotic building blocks. *Nat Chem.* 2020; 12 :1023–1028. [PubMed: 33093680]
53. Yew WS, et al. Evolution of enzymatic activities in the enolase superfamily: D-tartrate dehydratase from *Bradyrhizobium japonicum*. *Biochemistry.* 2006; 45 :14598–14608. [PubMed: 17144653]
54. Sagi VN, Punna V, Hu F, Meher G, Krishnamurthy R. Exploratory experiments on the chemistry of the “glyoxylate scenario”: formation of ketosugars from dihydroxyfumarate. *J Am Chem Soc.* 2012; 134 :3577–3589. [PubMed: 22280414]
55. Schrader T, et al. Vibrational relaxation following ultrafast internal conversion: comparing IR and Raman probing. *Chem Phys Lett.* 2004; 392 :358–364.
56. Ryseck G, et al. The excited-state decay of 1-methyl-2(*H*)-pyrimidinone is an activated process. *ChemPhysChem.* 2011; 12 :1880–1888. [PubMed: 21661090]
57. Haiser K, et al. Mechanism of UV-induced formation of Dewar lesions in DNA. *Angew Chem Int Ed.* 2012; 51 :408–411.
58. Satzger H, Zinth W. Visualization of transient absorption dynamics - towards a qualitative view of complex reaction kinetics. *Chem Phys.* 2003; 295 :287–295.
59. Dominguez PN, Himmelstoss M, Michelmann J, Lehner FT, Gardiner AT, Cogdell RJ, Zinth W. Primary reactions in photosynthetic reaction centers of *Rhodobacter sphaeroides*-Time constants of the initial electron transfer. *Chem Phys Lett.* 2014; 601 :103–109.
60. Gutierrez-Osuna R, Nagle HT, Schiffman SS. Transient response analysis of an electronic nose using multi-exponential models. *Sens Actuators B Chem.* 1999; 61 :170–182.
61. Buxton GV, Greenstock CL, Helman P, Ross AB. Critical Review of rate constants for reactions of hydrated electrons, hydrogen atoms and hydroxyl radicals in aqueous solution. *J Phys Chem Reference Data.* 1988; 17 :513–886.

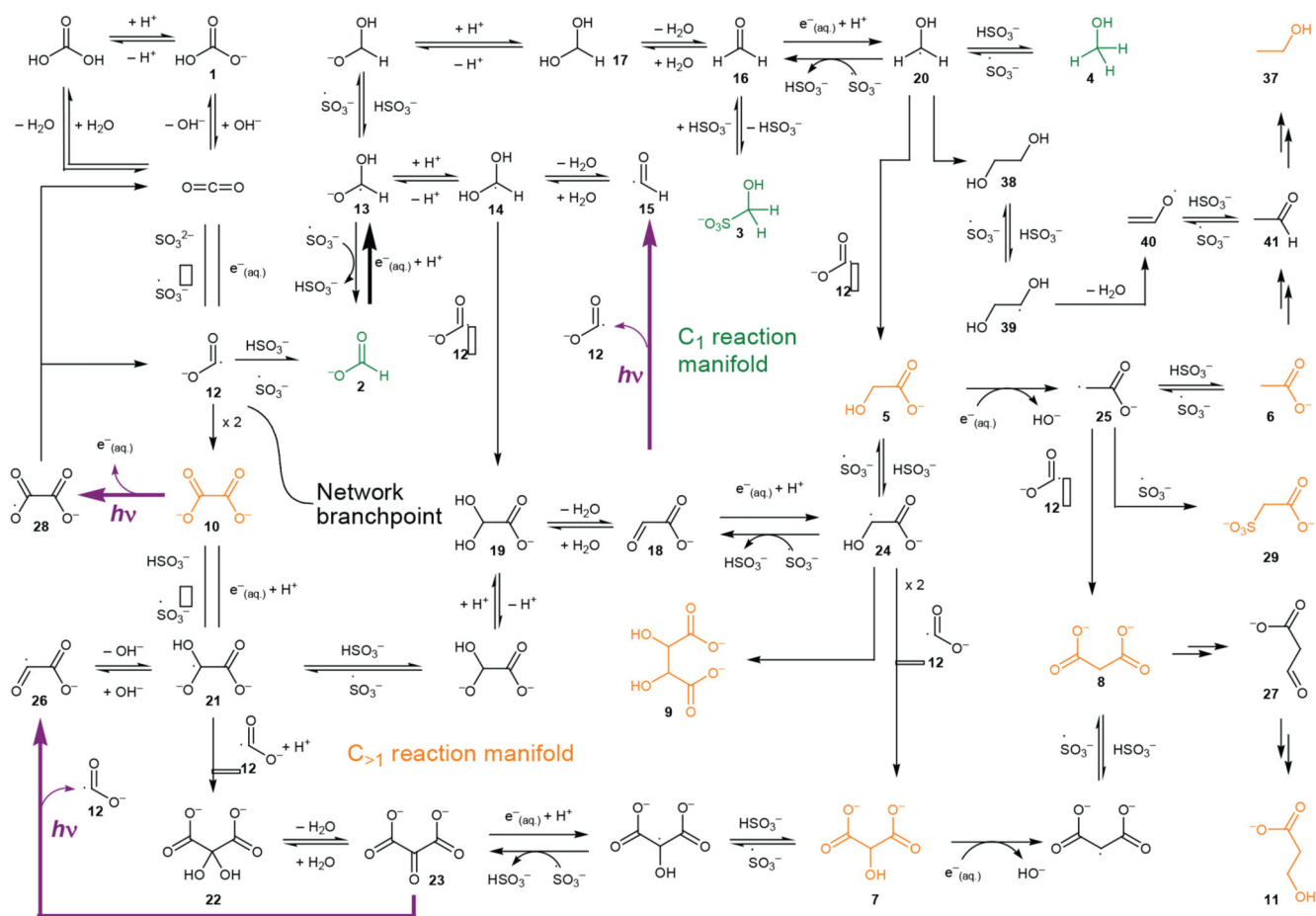


Fig. 1. Carboxysulfite photoredox reaction network starting from bicarbonate (HCO_3^-) 1. Starting in the top left, the reaction network starts with the addition of hydrated electrons (produced by photodetachment from sulfite) to CO_2 (blue) to give the carboxyl radical 12 after which point the network splits. Sequential reduction of the carboxyl radical 12 leads to the observed C₁ products (green) whilst dimerization of 12 to oxalate 10 initiates a path to C_{>1} products (orange). Various reactions enable crossing between the C₁ manifold and the C_{>1} manifold (the two manifolds are separated by a dashed line). The key oxidation of formate 2 back to the carboxyl radical 12 and the slow reduction of 2 that together divert flux from C₁ to C_{>1} products are highlighted (fuchsia arrows). Photochemical reactions of oxalate 10, glyoxylate 18 and mesoxalate 23 (purple arrows) also contribute to the network.

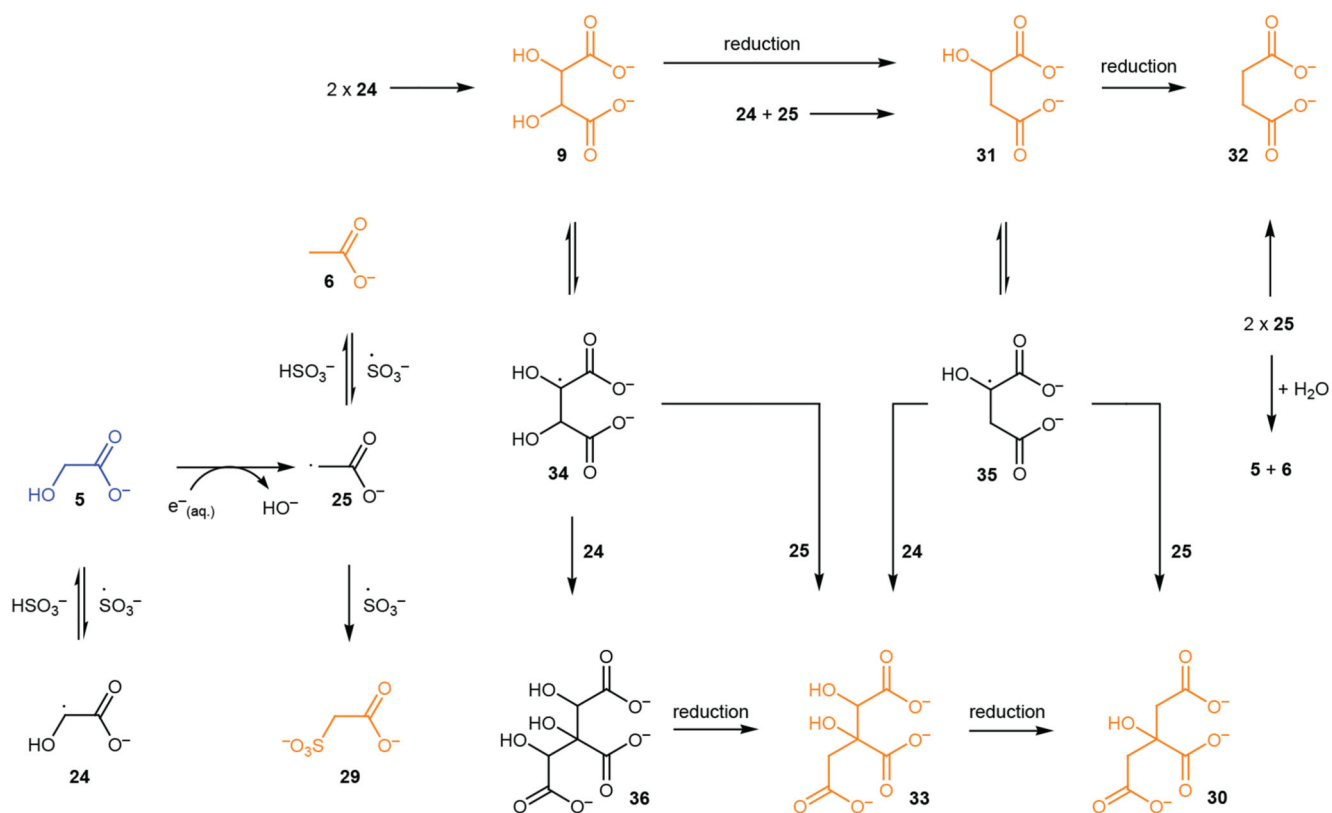
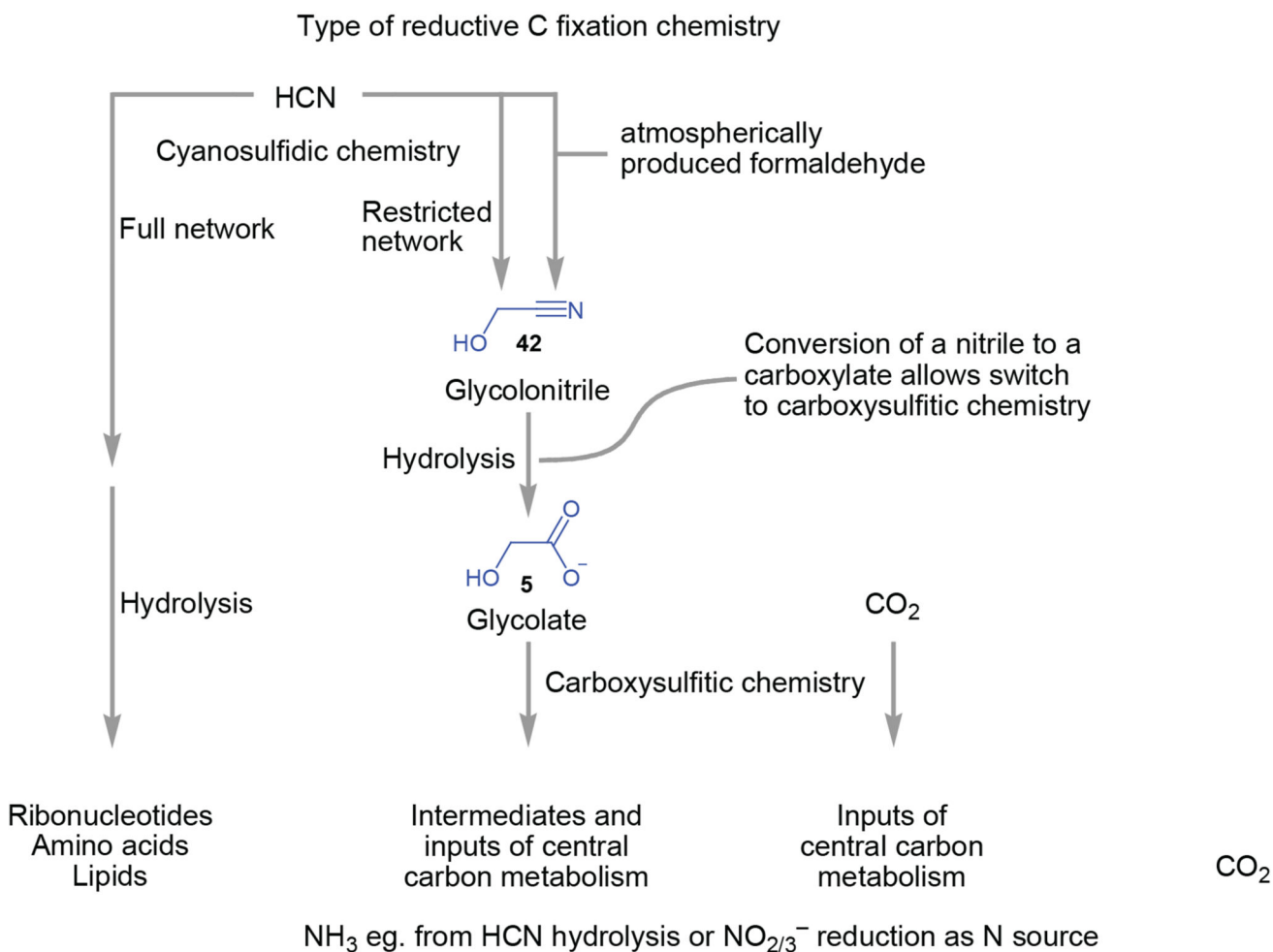


Fig. 2. Carboxysulfite photoredox reaction network starting from glycolate 5.

Glycolate **5** (blue) can be both oxidized by sulfite radicals and reduced by hydrated electrons to give the radicals **24** and **25** which then react further to give the observed products (orange). Recombination of two C₂ radicals (**24** and/or **25**) gives C₄ products (tartrate **9**, malate **31** and succinate **32**). Tartrate **9** and malate **31** can be oxidized by sulfite radicals giving C₄ radicals **34** and **35** and recombination of C₂ and C₄ radicals gives C₆ compounds (including the products hydroxycitrate **33** and citrate **30**). Reduction of dihydroxycitrate **36** and tartrate **9** provides additional reaction pathways to the C₆ and other C₄ products.



Environmentally available products of reductive C fixation chemistry

Fig. 3. Connections between environmental chemistry and the development of metabolism.

Progression from heterotrophy fed by photochemical products of inorganic carbon reduction to autotrophy as the available products of environmental chemistry become less complex. The preformed building blocks of RNA, peptides and lipids produced by cyanosulfidic chemistry provision the origin and early evolution of life^{5,52}, but gradually become depleted (fading of blue colour in timeline arrow) triggering the development of metabolism starting from simpler but more abundant products derived from glycolate **5** by cyanosulfidic chemistry (dark orange colour in timeline arrow). In turn, these materials become scarce (fading of orange colour in timeline arrow) and biology adapts to using carboxysulfitic products of CO_2 and eventually, CO_2 itself.